IEEE Access
Multidisciplinary | Rapid Review | Open Access Journal

Received February 24, 2019, accepted March 12, 2019, date of publication March 15, 2019, date of current version April 2, 2019.

Digital Object Identifier 10.1109/ACCESS.2019.2905247

A Nonlinear Flux Linkage Model for Bearingless Induction Motor Based on GWO-LSSVM

KE LI[1], GUOYU CHENG[1], XIAODONG SUN[2], (Senior Member, IEEE), AND ZEBIN YANG[1]
[1]School of Electrical and Information Engineering, Jiangsu University, Zhenjiang 212013, China
[2]Automotive Engineering Research Institute, Jiangsu University, Zhenjiang 212013, China

Corresponding author: Xiaodong Sun (xdsun@ujs.edu.cn)

This work was supported in part by the National Natural Science Foundation of China under Project 51875261 and Project 51475214, in part by the Natural Science Foundation of Jiangsu Province of China under Project BK20180046 and Project BK20170071, in part by the Qinglan Project of Jiangsu Province, in part by the Key Project of Natural Science Foundation of Jiangsu Higher Education Institutions under Project 17KJA460005, in part by the Six Categories Talent Peak of Jiangsu Province under Project 2015-XNYQC-003 and Project 2016-GDZB-096, in part by the 333 Project of Jiangsu Province under Project BRA2017441, and in part by the Priority Academic Program Development of Jiangsu Higher Education Institutions (PAPD).

ABSTRACT The flux-linkage characteristics of bearingless induction motors (BIMs) are nonlinear, and the models established by the general analytical method cannot accurately reflect the actual characteristics of BIMs. Thus, a novel method for nonlinear modeling of BIM flux linkage is proposed in this paper. The main objective of this method is to improve the accuracy of the flux linkage model based on the least square support vector machine (LSSVM) technique by applying the gray wolf optimization (GWO) algorithm to determine the optimal kernel parameter and regularization parameter of the LSSVM automatically. In this method, all BIMs flux linkage data are obtained from the finite-element method. In this paper, the relationship between input and output of the nonlinear flux linkage model is studied, and the precision model of GWO-LSSVM flux linkage is obtained. The simulation results demonstrate that the GWO-LSSVM model has high prediction accuracy and strong prediction ability. In addition, the GWO-LSSVM model is compared with other models. From this simulation comparison, it can be concluded that GWO-LSSVM modeling has the characteristics of higher accuracy.

INDEX TERMS Bearingless induction motor, gray wolf optimization, least squares support vector machine, nonlinear model, finite element analysis.

I. INTRODUCTION

In modern industrial production, such as high-speed machine tools, turbo-molecular pumps, centrifuges, compressors, electromechanical energy storage and some military fields, there is an increasing demand for high-speed drive performance of motors. Therefore, high-speed ultra-fine processing technology has become the most important part of advanced manufacturing technology [1]–[3]. When the rotor is running at high speed, the frictional resistance caused by the mechanical bearing increases, and the wear is intensified, resulting in heat generation of the motor. This reduces the operating efficiency of the motor, shortens the service life of the motor bearing, and increases the burden on the maintenance of the motor bearing. Because of the limitations of mechanical bearings, ordinary motors cannot operate normally in ultra-high-speed working environments [4], [5]. The bearingless motor is an emerging model of suspension motor that has developed rapidly in recent years. The bearingless motor not only has the characteristics that the rotor does not need mechanical bearing support during the operation, but also inherits the characteristics of non-lubrication, no wear and no mechanical noise of the magnetic bearing motor [6]. In terms of structure, the bearingless motor has a certain similarity with the related structure of the magnetic bearing and the AC motor [7]. The windings generating the suspension force are superimposed on the stator of the motor, so that the suspension force winding and the armature winding of the motor are combined into a whole [8]. The basic principle of a bearingless motor can be realized in various conventional motors, such as induction motors, reluctance motors, permanent magnet motors, etc [9]–[12]. Among the various types of bearingless motors, the bearingless induction motor (BIM) has many merits such as simple construction, low cost and

The associate editor coordinating the review of this manuscript and approving it for publication was M. A. Hannan.

high mechanical strength, which has attracted extensive attention of scholars. It is one of the earliest and most popular types of bearingless motors [13], [14].

A portion of the air gap magnetic field of the BIM is generated based on the torque winding of the original induction motor. Another portion of the air gap magnetic field is generated by the introduction of the current into the suspension force winding [15], [16]. The two magnetic fields are superimposed on each other, so the air gap magnetic field distribution is very complex, which leads to the serious nonlinear characteristics of the magnetic linkage of the BIM. In order to realize the steady suspension and operation of BIM, the real-time control of electromagnetic torque and radial suspension forces which are obtained by setting the partial derivatives of the magnetic energy according to the virtual displacement method are indispensable [17]. However, the magnetic energy is obtained by the inductance matrix of the flux linkage and the winding. Thus, obtaining an accurate flux linkage model is essential to accurately describe the electromagnetic and mechanical relationships of the BIM. Traditional analytical methods cannot express their real qualities in mathematical modeling, affecting the control precision and running performance of the BIM [18]. The method presented in this paper effectively compensates for these defects.

In recent years, the neural network has been successfully used to predict the accuracy of nonlinear modeling [19]. However, in the practical application, when the neural network is in the modeling process, it often encounters the problems of overfitting and local optimization [20], [21]. In order to overcome the shortcomings of neural networks, the support vector machine (SVM) has been developed and widely used. SVM is a new machine learning algorithm based on statistical learning theory and structural risk minimization principle [22]. In the limited sample information, the best compromise between the model complexity and the ability to identify samples is achieved to obtain the expected generalization ability. SVM has made great progress in the identification, classification and regression analysis of linear and nonlinear systems. It has the advantages of no dimensionality disaster and avoiding local minima and better generalization performance [23], [24]. However, the major drawback of SVM is the need to solve quadratic programming problems in practical applications. In order to solve the above problem of SVM, least square support vector machines (LSSVMs) have been developed. Compared with the SVM algorithm, the LSSVM algorithm uses the square term in the optimization index, changes the inequality constraint to the equality constraint, and transforms the quadratic programming problem into a linear equation solving problem, which simplifies the calculation [25]. However, during the modeling process, the key parameters in the LSSVM cannot be effectively optimized, which will not achieve the desired results [26]. The paper uses the gray wolf optimization (GWO) algorithm to solve this knotty optimization problem [27].

Mirjalili *et al.* [28] put forward GWO in 2014, which is a new swarm intelligence optimization algorithm. This algorithm is derived from the simulation of the predation behavior of the gray wolf population. The goal of optimization is achieved through the tracking, enclosing, and hunt the prey by the wolves. The GWO algorithm has the characteristics of simple principle, easy implementation and strong global search ability [29]. Compared with some proposed intelligent optimization algorithms, such as genetic algorithms (GA) and particle swarm optimization (PSO), GWO has significant advantages in convergence speed and solution accuracy. At present, it has been successfully applied in the fields of job shop scheduling, engineering optimization, support vector machine classification and economic dispatch assignment, effectively solving a variety of optimization problems. Therefore, GWO algorithm has a broader application prospect.

In [30], in order to develop a new and effective prediction system, this study explores the full potential of SVM by using the improved GWO strategy. An improved GWO algorithm is proposed to identify the most recognizable features of the main prediction. Firstly, the PSO algorithm is used to generate diversified initial positions, and then the current position of the population in the discrete search space is updated by GWO, so that the optimal feature subset based on SVM is obtained to achieve better classification. In [31], from the perspective of computation, it is proved that the reliability optimization problem of complex systems with nonlinear programming properties is a difficult problem in non-deterministic polynomials. In this work, few complex reliability optimization problems are solved by using a new natural-inspired meta-heuristic GWO algorithm. This comparative study shows that GWO is superior to some traditional optimization algorithms. In [32], an innovative fuzzy control system adjustment method is proposed, which uses the GWO algorithm to reduce the parameter sensitivity. The GWO algorithm is used to solve the optimization problem, where the objective function includes an output sensitivity function. The motivation for GWO is based on its low computational cost.

In this paper, the GWO is applied to optimize the kernel function parameter and the regularization parameter of LSSVM. The nonlinear modeling of the flux linkage model using the sampled data set obtained from the experimental prototype by the finite elements method is showed. The results show that the model can effectively reflect the magnetic properties of BIM. The paper is organized as follows. Section II introduces the nonlinear flux linkage modeling analysis. Section III shows the regression theory of LSSVM. Optimization of LSSVM parameters based on GWO is discussed in Section IV. The Section V describes the simulation research of the BIM nonlinear modeling based on GWO-LSSVM, followed by the conclusion in Section VI.

II. NONLINEAR FLUX LINKAGE MODELING ANALYSIS

BIM adds a set of the suspension winding to the stator slots of the original induction motor [33], [34]. Assume that the pole-pair numbers of the torque winding is P_t and the

magnetic field current frequency is ω_t. The pole-pair numbers of the other set of the suspension winding is P_s and its magnetic field current frequency is ω_s [35]. The magnetic fields produced by the torque winding and the suspension winding interact with each other, and then BIM produces a controllable suspension force. It should meet the following conditions

1) $P_t = P_s \pm 1$,
2) $\omega_t = \omega_s$
3) The magnetic fields generated by the windings have the same direction of rotation.

The nonlinear model function of the BIM flux linkage is as follows

$$\psi = \psi(\theta, i_t, i_s, l_0) \tag{1}$$

where ψ is the flux linkage of the BIM, θ is the rotor angle of BIM, i_t is the torque winding current, i_s is the suspension winding current and l_0 is the eccentric distance of the BIM rotor. As can be seen from the above equation, ψ is a nonlinear function composed of θ, i_t, i_s and l_0. In addition, the exact mathematical model of the flux linkage cannot be obtained from common analytical methods [36]. Therefore, this paper adopts the GWO to optimize the parameters in the LSSVM, and establishes the exact nonlinear model of the flux linkage.

III. REGRESSION THEORY OF LSSVM

SVM is a new and potential classification technology proposed by Vapnik and Corinna Cortes. The role is to solve the convex optimization problem [37]. LSSVM is an extension of SVM. The inequality constraint is replaced by equality constraint, avoiding solving the quadratic programming problem. The LSSVMs proposed by Khalil and El-Bardini [38] and Suykens *et al.* [39] can solve the linear KKT system. In this section, the regression theory of LSVSVM is briefly introduced.

The LSSVM problem can be described as follow, given the training set of l group data $\{x_i, y_i\}_{i=1}^{l}$, Among them, $x_i \in R^n$ is the input data, $y_i \in R$ is the output data. The LSSVM model is expressed in the feature space as the following function

$$y(\boldsymbol{x}) = w^T \boldsymbol{\Phi}(\boldsymbol{x}) + b \tag{2}$$

where $w \in R^H$ is a weight vector, the nonlinear mapping function Φ: $R^n \rightarrow R^H$ maps the input space to the high dimensional Hilbert space, and $b \in R$ is a bias term. Note that the dimension of feature space cannot be infinite when it is not specified. Although LSSVM can be used to estimate functions, the optimization problem is described below

$$\min J(w, \xi) = \frac{1}{2}\|w\|^2 + \frac{1}{2}\gamma \sum_{i=1}^{l} \xi_i^2 \tag{3}$$

Subject to the equality constraints

$$y_i = w^T \Phi(x_i) + b + \xi_i \quad i = 1, \ldots, l \tag{4}$$

where J is the objective function, γ is the regularization parameter and ξ_i is the relaxation factor. LSSVM defines a loss function that is different from standard SVM. The inequality constraints are changed to equality constraints, and w can be obtained from the dual space. In order to deal with the optimization problem of formula (3), the Lagrange function is established as

$$L(w, b, \xi, \alpha) = J(w, \xi) - \sum_{i=1}^{l} \alpha_i [w^T \Phi(x_i) + b + \xi_i - y_i] \tag{5}$$

where $\alpha = (\alpha_1, \alpha_2, \alpha_3, \ldots \alpha_l)^{\mathrm{T}}$ is a vector with a Lagrange multiplier, which is also called a support vector.

According to the KKT optimal condition, the calculated method is expressed as

$$\begin{cases} \dfrac{\partial L}{\partial w} = 0 \rightarrow w = \sum\limits_{i=1}^{l} \alpha_i \Phi(x_i) \\ \dfrac{\partial L}{\partial b} = 0 \rightarrow \sum\limits_{i=1}^{l} \alpha_i = 0 \\ \dfrac{\partial L}{\partial \xi_i} = 0 \rightarrow \alpha_i = \gamma \xi_i \quad i = 1, 2, \ldots l \\ \dfrac{\partial L}{\partial \alpha_i} = 0 \rightarrow w^{\mathrm{T}} \Phi(x_i) + b + \xi_i - y_i = 0 \end{cases} \tag{6}$$

After eliminating variables ξ_i and w by replacement, the optimization problem can be transformed into solving the following linear equations

$$\begin{bmatrix} 0 & 1_{l\times 1}^{\mathrm{T}} \\ 1_{l\times 1} & \Omega + \gamma^{-1} I \end{bmatrix} \begin{bmatrix} b \\ \alpha \end{bmatrix} = \begin{bmatrix} 0 \\ y \end{bmatrix} \tag{7}$$

where $y = [y_1, y_2, y_3, \cdots y_l]^T$, $1_{l\times 1} = [1, 1, \cdots 1]^T$, $I = diag[1, 1, \cdots 1]$, $\Omega = \left\{\Omega_{ij}\right\}_{l\times l}$, and $\Omega_{ij} = \Phi(x_i)\Phi(x_j)$, $i = 1, 2, 3, \cdots l$. The kernel function $K(x_i, x) = \Phi^T(x_i) \cdot \Phi(x)$ is defined as a symmetric function satisfying the Mercer theory. The common kernel function forms are linear, radial basis, polynomial and so on. Since the radial basis kernel function can make the classifier correctly predict the unknown data with high precision, the kernel function of this paper selects the following radial basis kernel function

$$K\ (x_i,\ x) = \exp\left(\frac{-|x_i - x|^2}{2\sigma^2}\right) \tag{8}$$

where σ is a constant defining the kernel width. Then we can obtain the decision function of LSSVM regression as follows

$$y(x) = \sum_{i=1}^{l} \alpha_i K(x_i, x) + b \tag{9}$$

It can be seen that in order to achieve the best predictive performance of LSSVM, it is important to optimize the regularization parameter γ and the kernel function parameter σ. The regularization parameter γ mainly controls the trade-off between the smoothness of the function and the accuracy of the approximation error. The kernel parameter σ primarily affects the distribution complexity of the sample data in the high dimensional feature space. Therefore, the GWO method is introduced to optimize the parameters (γ, σ) of the LSSVM to improve the generalization ability.

IV. OPTIMIZATION OF LSSVM PARAMETERS BASED ON GWO

A. GWO ALGORITHM

The Gray Wolf Optimization Algorithm (GWO) is a biological heuristic optimization algorithm whose essence is to imitate the social hierarchy and hunting nature of the Gray Wolf family. Gray wolves are social animals that establish a strict gray wolf pyramid level [40], [41].

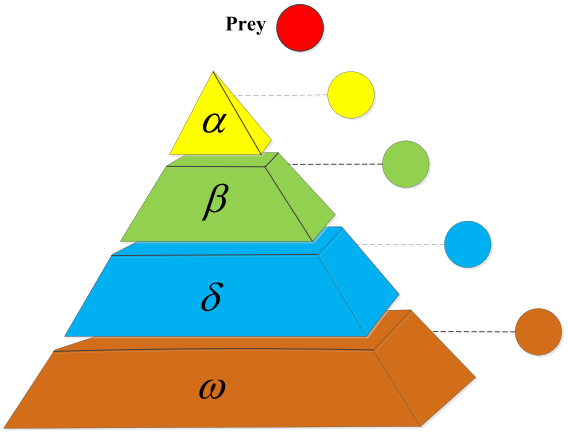

FIGURE 1. Social hierarchy of gray wolves.

From Figure 1, the social priority of the gray wolves is shown. The alpha (α) wolves, who are at the top of the pyramid, have supreme authority and lead other wolves. The α wolves are primarily responsible for predation and decision making, and other wolves must follow their orders. The beta (β) wolves, who are at the second layer of the pyramid, are second only to the α wolves. The β wolves are mainly responsible for assisting the α wolves in making decisions. The β wolves can control other individuals and feedback information about other wolves to the α wolves. The delta (δ) wolves, at the third layer of the pyramid, are mainly responsible for decision implementation of α wolves and β wolves. The status of δ wolves is higher than that of ω wolves. The omega (ω) wolves, at the bottom of the pyramid, are mainly responsible for helping to capture their prey. In GWO, the α wolves lead gray wolves to search and catch prey. When the wolves are very small from the range of prey, the α wolves command the β and δ wolves to siege the prey and let the surrounding ω wolves track and hunt until they finally succeed in capturing their prey.

For the mathematical modeling of the GWO algorithm, the hunting behavior of the gray wolf is simulated. Figure 2 shows the location update of the gray wolves. We need to randomly produce a pack of wolves in the search area. The wolves with a higher social hierarchy search for estimate the location of the prey. The wolves with the lowest priority are instructed to approach the prey and surround the prey, eventually capturing it successfully.

The modeling of GWO is as follows: in a K-dimensional search space, a group with N wolves is generated. After

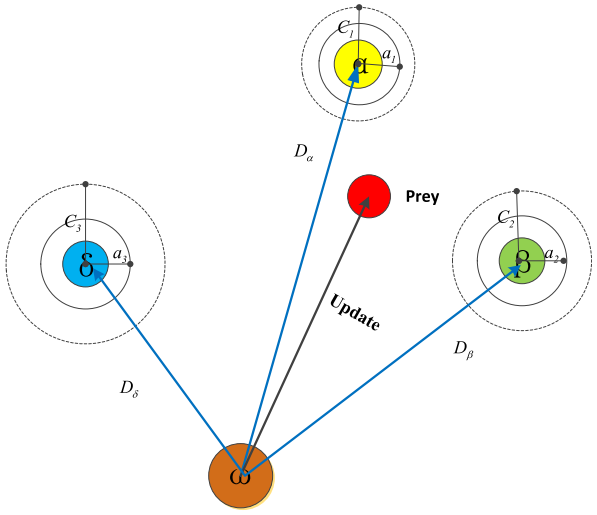

FIGURE 2. Gray wolf position update.

determining the position of the prey, the wolves first surround the prey. In the process, the distance between the prey and the gray wolves can be expressed as

$$\vec{D} = |\vec{C} \cdot \vec{X}_p(t) - \vec{X}(t)| \tag{10}$$

$$\vec{X}(t+1) = \vec{X}_p(t) - \vec{A} \cdot \vec{D} \tag{11}$$

where t represents the number of iterations, $\vec{X}$ is the current position vector for the gray wolves after t iterations, and $\vec{X}_p$ is the current position vector of the prey after t iterations. In every case of a metaheuristic algorithm, a random walk will be incorporated to find the global optimum solution with most accuracy or also closer to the expected solution. In GWO, the random is incorporated through the coefficient vectors given by the following equations:

$$\vec{A} = 2\vec{a} \cdot \vec{r}_1 - \vec{a} \tag{12}$$

$$\vec{C} = 2 \cdot r_2 \rightarrow \tag{13}$$

where $\vec{r}_1$ and $\vec{r}_2$ are random vectors in [0, 1]. With the increase of iteration time, $\vec{a}$ is linearly decreased from 2 to 0. Therefore, the value of $\vec{A}$ also randomly varies between [-a, a]. Moreover, when the random value of $\vec{A}$ is in [1, +1] the gray wolves will attack the prey, in dicating that the next location of the wolves will be closer to the prey. In the process of hunting, the function of $\vec{C}$ is seen as the effect of an obstacle approaching the prey in nature.

Surrounding the prey in the GWO algorithm is an important stage in the hunting process, which provides the best solution for moving to the prey in the search space. The simulated whole group of wolves was led by the α wolves. In each iteration, we can achieve the location of the α, β, and δ wolves, and force the lowest level wolves to update their location. The following equations illustrate the mathematical representation of such hunting actions:

$$\vec{D}_\alpha = |\vec{C}_1 \cdot \vec{X}_\alpha - \vec{X}| \tag{14}$$

$$\vec{D}_\beta = |\vec{C}_2 \cdot \vec{X}_\beta - \vec{X}| \tag{15}$$

$$\vec{D}_\delta = |\vec{C}_3 \cdot \vec{X}_\delta - \vec{X}| \quad (16)$$
$$\vec{X}_1 = \vec{X}_\alpha - \vec{A}_1 \cdot (\vec{D}_\alpha) \quad (17)$$
$$\vec{X}_2 = \vec{X}_\beta - \vec{A}_2 \cdot (\vec{D}_\beta) \quad (18)$$
$$\vec{X}_3 = \vec{X}_\delta - \vec{A}_3 \cdot (\vec{D}_\delta) \quad (19)$$
$$\vec{X}(t+1) = \frac{\vec{X}_1 + \vec{X}_2 + \vec{X}_3}{3} \quad (20)$$

In summary, the α, β, and δ wolves are gained by calculating the corresponding fitness, and the best three solutions can be used to estimate the possible location of the prey. The method for updating the location of the other wolves is shown in equations (14)–(20).

B. THE COMPUTATIONAL COST

An interesting part of using the GWO is the computational cost. In terms of function optimization, GWO has obvious advantages compared with other cluster intelligent optimization algorithms [42]. The artificial bee colony (ABC) optimization algorithm, simulated annealing (SA) algorithm and GWO are discussed to compare the running time. The ABC algorithm is also a novel optimization algorithm proposed in recent years. According to the related literature, its performance is better than traditional optimization algorithms such as genetic algorithms (GA) and particle swarm optimization (PSO). Then, the above three optimization algorithms are used to optimize formula (9).

The method of collecting data is the average running time of the algorithm running 30 times independently. The maximum number of iterations is used as the algorithm termination condition, and the population size of each algorithm is the same, that is, the maximum function evaluation times are the same. When the computational time of the function is the same, the different running time can reflect the difference of the structure of each algorithm. The running times of ABC, SA and GWO are 0.939s, 1.104s and 0.848s, respectively. It can be concluded that the selected GWO has certain advantages in terms of computational cost. The results show that compared with the other two algorithms, GWO has a faster speed of optimization. The ABC and SA use serial computing to calculate fitness function values, while the GWO design can adopt the large-scale operation mode, which greatly improves the running speed of the algorithm. Social hierarchy plays an important role in the process of wolves effectively catching prey, which can accelerate the convergence speed and reduce the calculation cost. In summary, GWO is used to optimize the parameters in the LSSVM.

C. GWO-LSSVM

It is well known that the values of the regularization parameter γ and the kernel parameter σ directly affect the accuracy of the LSSVM prediction model [43]. Therefore, in this paper, the above two parameters of LSSVM are optimized by GWO method. The specific steps of GWO-LSSVM are summarized as follows:

Step 1: Set the parameters range associated with GWO, γ and σ in the LSSVM.

Step 2: Initialize the wolf population and use γ and σ to describe the location vector for each wolf.

Step 3: Learn the training data and the test data using the initialized LSSVM, and then evaluate the fitness value of the individual gray wolf.

Step 4: Classify gray wolves to identify the location of α wolves, β wolves, δ wolves and ω wolves.

Step 5: Accurately update the location of each wolf in order to create new populations, evaluate the fitness value, and compare it with the previous iteration.

Step 6: Confirm if the maximum iteration is achieved, and if so, end the iteration and get the optimized γ and σ. Otherwise, skip to step 3 to optimize the parameters continuously.

Step 7: Employ the optimized γ and σ of LSSVM to set up the prediction model, and predict the test data.

The flowchart of the GWO-LSSVM model is shown in Fig.3.

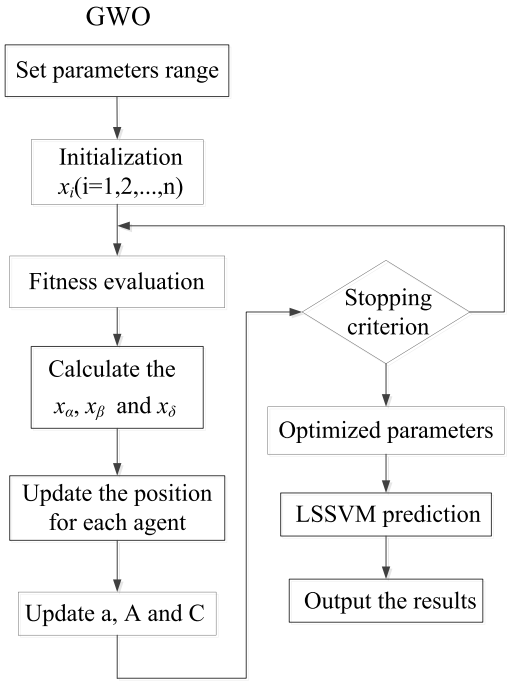

FIGURE 3. Flowchart of the GWO-LSSVM model.

V. NONLINEAR MODELING OF BIM BASED ON LSSVM

A. INTRODUCTION TO BIM SPECIFICATIONS

In this paper, Matlab R2016a is used to realize the nonlinear modeling of BIMs flux linkage by GWO-LSSVM algorithm. A BIM nonlinear model with rated power of 3kW and rated voltage of 380V is obtained with GWO-LSSVM. Due to the limited experimental conditions, there is no corresponding experimental equipment to measure the flux linkage. Therefore, when researching the method of BIM nonlinear modeling, the flux linkage values under three conditions are obtained by finite element analysis. However, the model built

will lay a solid foundation for the actual magnetic flux modeling in the future, creating conditions for further improving system performance and real-time control [44], [45]. The main specifications of BIM are shown in Table 1.

TABLE 1. Motor specifications and major dimensions.

Items	Values
Rated frequency	380V
Outer stator diameter	96mm
Inner stator diameter	50mm
Rotor outer diameter	49.4mm
Length of stator core	47mm
Coercive force	900KA/m^{-1}
Stator slots number	24
Rotor slots number	30
Pole pairs of torque windings	2
Pole pairs of suspension windings	1
Coil turns number of torque windings	110
Coil turns number of suspension windings	110

B. ANALYSIS OF GWO-LSSVM MODELING RESULTS

In the simulation, $\varepsilon_{\mathrm{RMSE}}$ is defined as the root mean square error and $\varepsilon_{\mathrm{MAXE}}$ is defined as the maximum absolute error. $\varepsilon_{\mathrm{RMSE}}$ and $\varepsilon_{\mathrm{MAXE}}$ are used as indicators for evaluating the predictive performance of the flux linkage model. $\varepsilon_{\mathrm{RMSE}}$ is used as the objective function of GWO algorithm

$$\varepsilon_{\mathrm{RMSE}} = \sqrt{\frac{1}{l}\sum_{i=1}^{l}(y_i - \hat{y}_i)^2} \tag{21}$$

where y_{i} and $\hat{y}_i$ are the actual value and the output value respectively, $i = 1, 2, 3 \cdots l$. When $\varepsilon_{\mathrm{RMSE}}$ reaches the minimum value, the regularization parameter γ and the kernel function parameter σ achieve the optimal parameters

Another parameter $\varepsilon_{\mathrm{MAXE}}$ is defined as follows

$$\varepsilon_{\mathrm{MAXE}} = \max_{j=1}^{N} |y_j - \hat{y}_j| \tag{22}$$

where y_j and $\hat{y}_j$ are the actual value and the output value respectively, $j = 1, 2, 3 \cdots N$.

Table 2 shows the selected parameters of the GWO algorithm. Before starting the optimization process, some parameters of GWO should be selected. The size of the wolves will directly affect the timing and accuracy of the optimization. More wolves will consume more time, but too few wolves may not find the best gain matrix. According to the information contained in the wolves, the number of wolves is chosen to be 30. To ensure that the gain matrix can be selected over a wide range of values, the upper and lower limits are chosen to be 1e06 and 1e-03. The maximum number of iterations is a key parameter in the simulation and must be carefully chosen.

The optimal values of LSSVM parameters optimized by GWO are $\gamma = 1000$ and $\sigma = 4.2$. To compare models performance, the LSSVM, GWO-LSSVM SA-LSSVM and ABC-LSSVM are used to set up the nonlinear model of the BIM flux linkage. When the number of maximum iterations is set to 40, $\varepsilon_{\mathrm{RMSE}}$ and $\varepsilon_{\mathrm{MAXE}}$ of the selected test data are

TABLE 2. Selected parameters of GWO.

Items	Values
Number of wolves	30
Maximum iterations	40
Upper bounds	1e06
Lower bounds	1e-03

TABLE 3. Comparison of prediction effects between four models.

	$\varepsilon_{\mathrm{RMSE}}$	$\varepsilon_{\mathrm{MAXE}}$
LSSVM	9.21e-04	2.53e-04
GWO-LSSVM	2.63e-04	0.64e-04
SA-LSSVM	4.85e-04	1.37 e-04
ABC-LSSVM	2.94e-04	0.86 e-04

compared. The result is shown in Table 3. After the LSSVM is used to model the BIM flux linkage, the values of $\varepsilon_{\mathrm{MAXE}}$ and $\varepsilon_{\mathrm{MAXE}}$ are large, indicating that the model's prediction performance is poor. Using GWO-LSSVM can reduce the error by three to four times. The values of $\varepsilon_{\mathrm{RMSE}}$ and $\varepsilon_{\mathrm{MAXE}}$ of flux linkage model established by SA-LSSVM are also relatively large, and the prediction performance is not ideal. In addition, it is worth mentioning that ABC-LSSVM modeling has high prediction accuracy, but slightly inferior to GWO-LSSVM modeling. It can be seen that the nonlinear model of the BIM flux linkage has better fitting ability and prediction accuracy by using GWO algorithm to optimize LSSVM parameters.

The SA algorithm is a relatively traditional optimization algorithm, and its idea has been proposed as early as 1953. The ABC algorithm is also a new optimization algorithm proposed in recent years, which has good optimization performance. The GWO algorithm has the characteristics of simple operation, less adjustment parameters, and easy programming. The iterative convergence of the three optimization algorithms is compared. Figure 4 shows the comparison of the iterative convergence performance of these algorithms. When the number of iterations using SA-LSSVM is 27, the fitness value tends to be stable. The number of iterations using ABC-LSSVM is 23, and the fitness value tends to be stable. However, the number of iterations using GWO-LSSVM is 20, and the line of fitness value tends to be smooth. From the comparison results, it can be found that the GWO-LSSVM

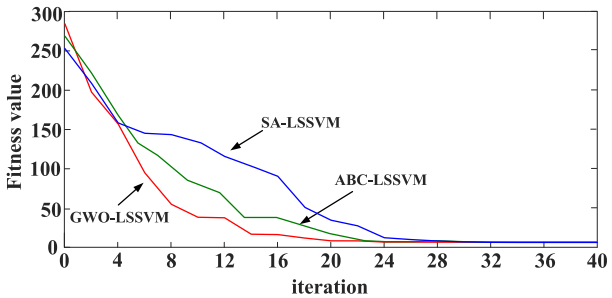

FIGURE 4. Comparison of iterative convergence.

model has higher convergence accuracy. Then, from table 3 and Figure 4, it can be concluded that GWO-LSSVM has better robustness, prediction accuracy and optimization speed.

In order to study the GWO-LSSVM model of the BIM flux linkage, the sample data is first collected from the finite element method. At each 5-degree rotor position, a set of data was measured and a total of 73 sets of data were measured. Among them, the 37 sets of flux linkage data for even rotor position angle numbers are used for training, and 36 sets of flux linkage data for odd rotor position angle are used for testing. In addition, the rotor angle θ, torque winding current i_t, suspension winding current i_s and rotor eccentricity l_0 are the inputs of GWO-LSSVM model, while the flux linkage of the BIM is the output of the model. So the nonlinear model of flux linkage is five-dimensional, but it cannot be expressed in a plane coordinate. In this paper, the relationship between variables and flux linkage is expressed in a two-dimensional coordinate plane.

The GWO-LSSVM model of the BIM flux linkage was established under three different conditions as follows. In the figure, the hollow dots and asterisks are represented as training data or test data, and the dotted lines are regarded as fitting output or predicting output. The following figures show the comparison of the training and test output results of the model, respectively. When the suspension force winding current i_s is fixed at 3A and the torque winding current i_t is 2A and 4A, the comparison results are shown in Fgures.5 and 6. Figure 5 shows the comparison between the training data value and the model output value (fitting value). Figure 6 shows the comparison between the testing data value and the model output value (predicting value). The current of suspension force winding is fixed, the current of torque winding increases from 2A to 4A, and the magnitude of flux linkage curve increases a lot. It can be seen from the figure below that when $i_s = 3$ and $i_t = 5$, the flux linkage is sinusoidal, while $i_s = 3$ and $i_t = 2$, the flux linkage has no rule of the former. BIM flux linkage is nearly sinusoidal, which can obtain stable suspension force. If the error of modeling is large, it will affect the control of suspension force. Therefore, it is very important to obtain

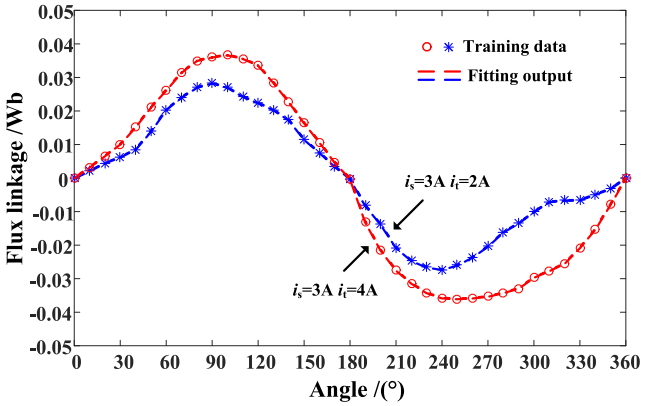

FIGURE 5. Comparison results of training data and fitting output.

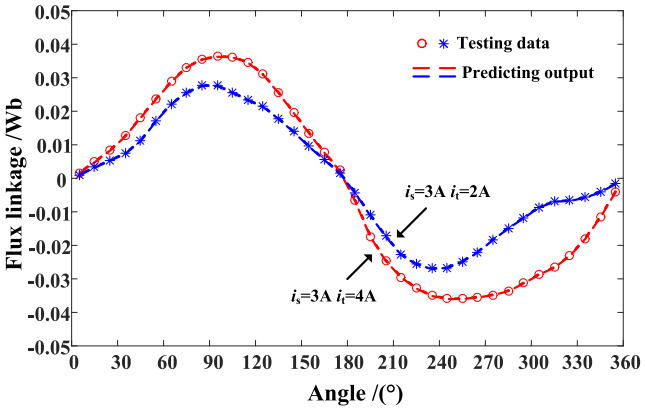

FIGURE 6. Comparison results of tested data and predicting output.

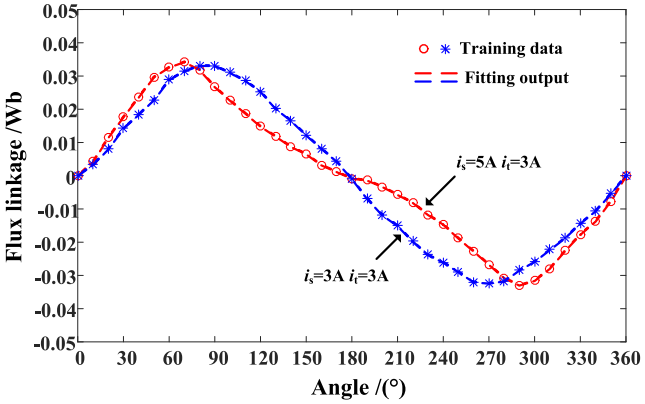

FIGURE 7. Comparison results of training data and fitting output.

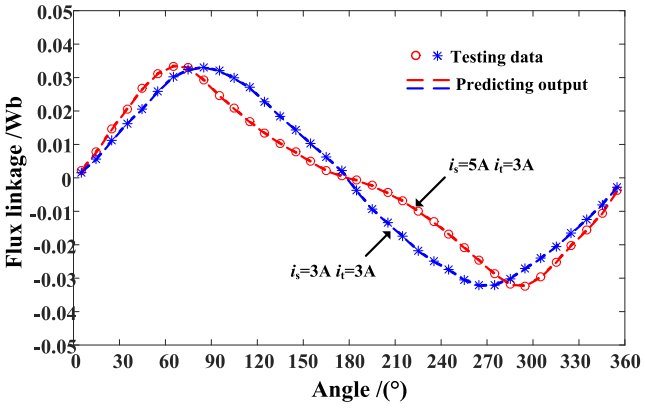

FIGURE 8. Comparison results of tested data and predicting output.

reliable flux model. The fitting and predicting values are in good agreement with the actual values, which shows that the model has high prediction accuracy. When the torque winding current i_t is fixed at 3A and the suspension force winding current i_s is 3A and 5A, the comparison results are shown in Figures.7 and 8. Figure 7 shows the comparison between the training data value and the fitting data value. Figure 8 shows the comparison between the testing data value and the predicting data value. When $i_s = 3$ and $i_t = 3$,

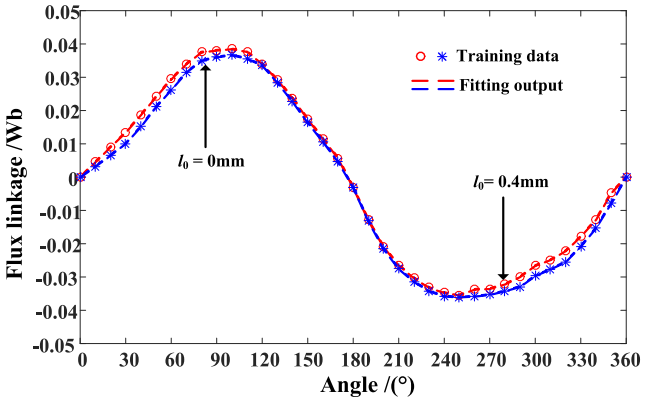

FIGURE 9. Comparison results of training data and fitting output.

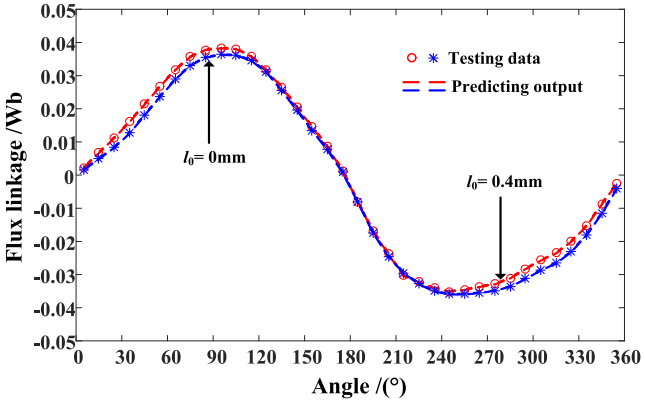

FIGURE 10. Comparison results of tested data and predicting output.

the flux linkage has a sinusoidal shape, and when $i_s = 5$ and $i_t = 3$, the flux linkage is not an ideal sinusoidal shape. The method of obtaining the flux linkage by GWO-LSSVM can also obtain good prediction performance under the condition that the flux linkage data is not ideal. The comparison results of the nonlinear flux linkage curves when the rotor is eccentrically 0.4 mm and the rotor is not eccentric are shown in Figures.9 and 10. Figure 9 shows the comparison between training data value and fitting output value. Figure 10 shows a comparison between testing data value and predicting output value. Due to the influence of gravity and eccentricity of the BIM rotor, the unilateral magnetic pull force will be caused. In order to ensure stable operation, a large enough suspension force is required to stably support the rotor. In other words, the radial suspension force generated by the suspension force winding current can overcome the unilateral magnetic pulling force. However, the winding current has not changed. Therefore, the following highly accurate rotor eccentric flux linkage model can be obtained.

It can be seen from the Figure5 to Figure 10 that the results of the fitting output and the predicting output are quite consistent with the data obtained by the finite element analysis. The root means square error of the test sample and the model test output is 0.000263, and the maximum absolute error is 0.000064, which indicates that the model has better robustness and prediction accuracy.

VI. CONCLUSION

A novel GWO-LSSVM modeling method is proposed in this paper. By this method, a nonlinear flux linkage model is introduced in the BIM flux linkage $\psi(\theta, i_t, i_s, l_0)$. Besides, the training data, the model does not need any knowledge of the magnetic characteristics of the motor. Therefore, this method is suitable for modeling of the BIM with strong nonlinear characteristics. The primary novelty is using the proposed GWO-based approach, which aims at optimizing the parameters of the LSSVM. From the simulation results, it can be concluded that the nonlinear model built by GWO-LSSVM has superior generalization ability, which makes the model have high precision and strong predictive ability. In addition, it is interesting to note that the modeling process and basic idea of the GWO-LSSVM model are universal and can be applied to nonlinear modeling of other types of bearingless motors.

COMPETING INTERESTS

The authors declare that they have no competing interests.

REFERENCES

[1] F. R. Ismagilov, N. Uzhegov, V. E. Vavilov, V. Bekuzin, and V. Ayguzina, "Multidisciplinary design of ultra-high-speed electrical machines," *IEEE Trans. Energy Convers.*, vol. 33, no. 3, pp. 1203–1212, Sep. 2018.

[2] D. Dietz, G. Messager, and A. Binder, "1 kW/60,000 min^{-1} bearingless PM motor with combined winding for torque and rotor suspension," *IET Electr. Power Appl.*, vol. 12, no. 8, pp. 1090–1097, 2018.

[3] Y. Le, J. Fang, and K. Wang, "Design and optimization of a radial magnetic bearing for high-speed motor with flexible rotor," *IEEE Trans. Magn.*, vol. 51, no. 6, pp. 1–13, Jun. 2015.

[4] X. Sun, Y. Shen, S. Wang, G. Lei, Z. Yang, and S. Han, "Core losses analysis of a novel 16/10 segmented rotor switched reluctance BSG motor for HEVs using nonlinear lumped parameter equivalent circuit model," *IEEE/ASME Trans. Mechatronics*, vol. 23, no. 2, pp. 747–757, Apr. 2018.

[5] M. Montazeri-Gh and M. Mahmoodi-K, "Development a new power management strategy for power split hybrid electric vehicles," *Transp. Res. D, Transp. Environ.*, vol. 37, pp. 79–96, Jun. 2015.

[6] H. S. Zad, T. I. Khan, and I. Lazoglu, "Design and analysis of a novel bearingless motor for a miniature axial flow blood pump," *IEEE Trans. Ind. Electron.*, vol. 65, no. 5, pp. 4006–4016, May 2018.

[7] X. Sun, B. Su, L. Chen, Z. Yang, X. Xu, and Z. Shi, "Precise control of a four degree-of-freedom permanent magnet biased active magnetic bearing system in a magnetically suspended direct-driven spindle using neural network inverse scheme," *Mech. Syst. Signal Process.*, vol. 88, pp. 36–48, May 2017.

[8] G. Sala *et al.*, "Space vectors and pseudoinverse matrix methods for the radial force control in bearingless multisector permanent magnet machines," *IEEE Trans. Ind. Electron.*, vol. 65, no. 9, pp. 6912–6922, Sep. 2018.

[9] W. Bu, X. Zhang, and F. He, "Sliding mode variable structure control strategy of bearingless induction motor based on inverse system decoupling," *IEEJ Trans. Electr. Electron. Eng.*, vol. 13, pp. 1052–1059, Jul. 2018.

[10] J.-H. Kim and R.-Y. Kim, "Sensorless direct torque control using the inductance inflection point for a switched reluctance motor," *IEEE Trans. Ind. Electron.*, vol. 65, no. 12, pp. 9336–9345, Dec. 2018.

[11] J. Huang, B. Li, H. Jiang, and M. Kang, "Analysis and control of multiphase permanent-magnet bearingless motor with a single set of half-coiled Winding," *IEEE Trans. Ind. Electron.*, vol. 61, no. 7, pp. 3137–3145, Jul. 2014.

[12] X. Sun *et al.*, "Performance analysis of suspension force and torque in an IBPMSM with V-shaped PMs for flywheel batteries," *IEEE Trans. Magn.*, vol. 54, no. 11, Nov. 2018, Art. no. 8105504.
[13] Z. Shi *et al.*, "Torque analysis and dynamic performance improvement of A PMSM for EVs by skew angle optimization," *IEEE Trans. Appl. Supercond.*, vol. 29, no. 2, Mar. 2019, Art. no. 0600305. doi: 10.1109/TASC.2018.2882419.
[14] X. Sun *et al.*, "Suspension force modeling for a bearingless permanent magnet synchronous motor using maxwell stress tensor method," *IEEE Trans. Appl. Supercond.*, vol. 26, no. 7, Oct. 2016, Art. no. 0608705.
[15] A. Sinervo and A. Arkkio, "Rotor radial position control and its effect on the total efficiency of a bearingless induction motor with a cage rotor," *IEEE Trans. Magn.*, vol. 50, no. 4, pp. 1–9, Apr. 2014.
[16] X. Sun *et al.*, "Performance improvement of torque and suspension force for a novel five-phase BFSPM machine for flywheel energy storage systems," *IEEE Trans. Appl. Supercond.*, vol. 29, no. 2, Mar. 2019, Art. no. 0601505. doi: 10.1109/TASC.2019.2893295.
[17] T. Katou, A. Chiba, and T. Fukao, "Magnetic suspension force in an induction bearingless motor with a squirrel cage rotor," *Electr. Eng. Jpn.*, vol. 159, pp. 77–87, May 2007.
[18] W. Bu, Z. Li, C. Lu, X. Wang, and J. Xiao, "Research on the least squares support vector machine displacement observer of a bearingless induction motor," *Trans. Inst. Meas. Control*, vol. 39, no. 5, pp. 688–697, 2015.
[19] X. Sun, L. Chen, H. Jiang, Z. Yang, J. Chen, and W. Zhang, "High-performance control for a bearingless permanent-magnet synchronous motor using neural network inverse scheme plus internal model controllers," *IEEE Trans. Ind. Electron.*, vol. 63, no. 6, pp. 3479–3488, Jun. 2016.
[20] D. Avola, L. Cinque, G. L. Foresti, M. R. Marini, and D. Pannone, "VRheab: A fully immersive motor rehabilitation system based on recurrent neural network," *Multimedia Tools Appl.*, vol. 77, no. 19, pp. 24955–24982, 2018.
[21] X. Sun, L. Chen, Z. Yang, and H. Zhu, "Speed-sensorless vector control of a bearingless induction motor with artificial neural network inverse speed observer," *IEEE/ASME Trans. Mechatronics*, vol. 18, no. 4, pp. 1357–1366, Aug. 2013.
[22] G. W. Flake and S. Lawrence, "Efficient SVM regression training with SMO," *Mach. Learn.*, vol. 46, nos. 1–3, pp. 271–290, 2002.
[23] K. Salahshoor, M. Kordestani, and M. S. Khoshro, "Fault detection and diagnosis of an industrial steam turbine using fusion of SVM (support vector machine) and ANFIS (adaptive neuro-fuzzy inference system) classifiers," *Energy*, vol. 35, pp. 5472–5482, Dec. 2010.
[24] A. J. Smola and B. Schölkopf, "A tutorial on support vector regression," *Statist. Comput.*, vol. 14, no. 3, pp. 199–222, Aug. 2004.
[25] M. D. de Lima, N. L. Costa, and R. Barbosa, "Improvements on least squares twin multi-class classification support vector machine," *Neurocomputing*, vol. 313, pp. 196–205, Nov. 2018.
[26] Y. Shao, N. Deng, and Z. Yang, "Least squares recursive projection twin support vector machine for classification," *Pattern Recognit.*, vol. 45, no. 6, pp. 2299–2307, 2012.
[27] X.-Q. Bian, Q. Zhang, L. Zhang, and J. Chen, "A grey wolf optimizer-based support vector machine for the solubility of aromatic compounds in supercritical carbon dioxide," *Chem. Eng. Res. Design*, vol. 123, pp. 284–294, Jul. 2017.
[28] S. Mirjalili, S. M. Mirjalili, and A. Lewis, "Grey wolf optimizer," *Adv. Eng. Softw.*, vol. 69, pp. 46–61, Mar. 2014.
[29] R. A. Ibrahim, M. A. Elaziz, and S. Lu, "Chaotic opposition-based grey-wolf optimization algorithm based on differential evolution and disruption operator for global optimization," *Expert Syst. Appl.*, vol. 108, pp. 1–27, Oct. 2018.
[30] Y. Wei *et al.*, "An improved grey wolf optimization strategy enhanced SVM and its application in predicting the second major," *Math. Problems Eng.*, vol. 2017, Feb. 2017, Art. no. 9316713.
[31] A. Kumar, S. Pant, and M. Ram, "System reliability optimization using gray wolf optimizer algorithm," *Qual. Rel. Eng. Int.*, vol. 33, pp. 1327–1335, Nov. 2017.
[32] R.-E. Precup, R.-C. David, and E. M. Petriu, "Grey wolf optimizer algorithm-based tuning of fuzzy control systems with reduced parametric sensitivity," *IEEE Trans. Ind. Electron.*, vol. 64, no. 1, pp. 527–534, Jan. 2017.
[33] X. Sun, L. Chen, and Z. Yang, "Overview of bearingless permanent-magnet synchronous motors," *IEEE Trans. Ind. Electron.*, vol. 60, no. 12, pp. 5528–5538, Dec. 2013.
[34] Z. Yang, D. Zhang, X. Sun, and X. Ye, "Adaptive exponential sliding mode control for a bearingless induction motor based on a disturbance observer," *IEEE Access*, vol. 6, pp. 35425–35434, 2018.
[35] X. Sun, B. Su, L. Chen, Z. Yang, J. Chen, and W. Zhang, "Nonlinear flux linkage modeling of a bearingless permanent magnet synchronous motor based on AW-LSSVM regression algorithm," *Int. J. Appl. Electromagn. Mech.*, vol. 51, pp. 151–159, Jun. 2016.
[36] M. Manohar and S. Das, "Current sensor fault-tolerant control for direct torque control of induction motor drive using flux-linkage observer," *IEEE Trans. Ind. Informat.*, vol. 13, no. 6, pp. 2824–2833, Dec. 2017.
[37] V. Cherkassky and Y. Ma, "Practical selection of SVM parameters and noise estimation for SVM regression," *Neural Netw.*, vol. 17, no. 1, pp. 113–126, Jan. 2004.
[38] H. M. Khalil and M. El-Bardini, "Implementation of speed controller for rotary hydraulic motor based on LS-SVM," *Expert Syst. Appl.*, vol. 38, pp. 14249–14256, Oct. 2011.
[39] J. A. K. Suykens, J. Vandewalle, and B. De Moor, "Optimal control by least squares support vector machines," *Neural Netw.*, vol. 14, pp. 23–35, Jan. 2001.
[40] M. Fahad *et al.*, "Grey wolf optimization based clustering algorithm for vehicular ad-hoc networks," *Comput. Elect. Eng.*, vol. 70, pp. 853–870, Aug. 2018.
[41] V. Kamboj, "A novel hybrid PSO–GWO approach for unit commitment problem," *Neural Comput. Appl.*, vol. 27, pp. 1643–1655, Aug. 2016.
[42] A. Kaveh and P. Zakian, "Improved GWO algorithm for optimal design of truss structures," *Eng. Comput.*, vol. 34, pp. 685–707, Oct. 2018.
[43] M. S. Borujeni, M. Ghaderi-Zefrehei, F. Ghanegolmohammadi, and S. Ansari-Mahyari, "A novel LSSVM based algorithm to increase accuracy of bacterial growth modeling," *Iranian J. Biotechnol.*, vol. 16, no. 2, pp. 105–113, 2018.
[44] H. Chen, W. Yan, L. Chen, M. Sun, and Z. Liu, "Analytical polynomial models of nonlinear magnetic flux linkage for SRM," *IEEE Trans. Appl. Supercond.*, vol. 28, no. 3, Apr. 2018, Art. no. 5205307.
[45] X. Sun, Z. Shi, L. Chen, and Z. Yang, "Internal model control for a bearingless permanent magnet synchronous motor based on inverse system method," *IEEE Trans. Energy Convers.*, vol. 31, no. 4, pp. 1539–1548, Dec. 2016.

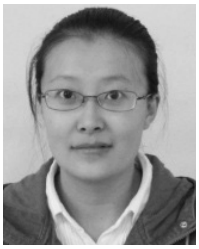

KE LI was born in Zhenjiang, Jiangsu, China, in 1982. She received the M.S. and M.Sc. degrees in control engineering from Jiangsu University, Zhenjiang, in 2003 and 2008, respectively, where she is currently pursuing the Ph.D. degree in control engineering.

She is currently an Associate Professor with the School of Electrical and Information Engineering, Jiangsu University. Her areas of interests include magnetic bearings, magnetic suspension (bearingless) motors, motor movement control, hybrid electric vehicles, and intelligent control.

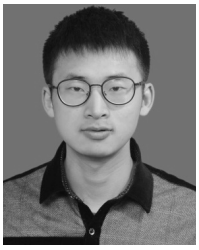

GUOYU CHENG was born in Huai'an, Jiangsu, China, in 1993. He received the B.S. degree from Jiangsu University, Zhenjiang, China, where he is currently pursuing the M.S. degree in control science and engineering with the School of Electrical and Information Engineering.

His current research interests include bearingless motors, motor drives, control electric vehicles, hybrid electric vehicles, and intelligent control of special motors.

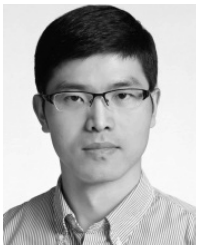

XIAODONG SUN (M'12–SM'18) received the B.Sc. degree in electrical engineering, and the M.Sc. and Ph.D. degrees in control engineering from Jiangsu University, Zhenjiang, China, in 2004, 2008, and 2011, respectively. From 2014 to 2015, he was a Visiting Professor with the School of Electrical, Mechanical, and Mechatronic Systems, University of Technology Sydney, Sydney, Australia. Since 2004, he has been with Jiangsu University, where he is currently a Professor with the Automotive Engineering Research Institute. His current teaching and research interests include electrical machines and drives, drives and control for electric vehicles, and intelligent control. He has authored or co-authored more than 90 refereed technical papers and one book and holds 45 patents in his areas of interest.

ZEBIN YANG received the B.Sc., M.Sc., and Ph.D. degrees in electrical engineering from Jiangsu University, Zhenjiang, China, in 1999, 2004, and 2013, respectively. From 2014 to 2015, he was a Visiting Scholar with the School of Electrical, Mechanical, and Mechatronic Systems, University of Technology Sydney, Sydney, Australia. He is currently a Professor with Jiangsu University. His main research interests include drives and control for bearingless motors, and magnetic levitation transmission technology.